Synthesisation of Zinc Oxide Nanowires via Hybrid Microwave-Assisted Sonochemical Technique at Various Microwave Power

Maryam Mohammad
Department of Physics, Faculty of Applied Sciences,
Universiti Teknologi MARA (UiTM) Perak Branch, Tapah Campus,
Tapah Road, 35400 Perak, MALAYSIA

Mohd Firdaus Malek[*]*, Muhammad Faizal Abd Halim,*
Nurul Zulaikha Mohammad Zamri, Mohamad Dzulfiqar Bakri,
Zuraida Khusaimi
NANO-SciTech Lab (NST), Centre for Functional Materials and
Nanotechnology (FMN), Institute of Science (IOS),
Faculty of Applied Sciences, Universiti Teknologi MARA (UiTM),
40450 Shah Alam, Selangor, MALAYSIA
[*]*mfmalek07@uitm.edu.my; mfmalek07@gmail.com*

Mohamad Hafiz Mamat, Mohamad Rusop Mahmood
NANO-ElecTronic Centre (NET), School of Electrical Engineering,
College of Engineering, Universiti Teknologi MARA (UiTM),
Shah Alam 40450, Selangor, MALAYSIA

Tetsuo Soga
Department Of Electrical and Mechanical Engineering,
Nagoya Institute of Technology, Showa-Ku, Gokiso-Cho, Nagoya, 466-8555,
JAPAN

ABSTRACT

Zinc oxide nanowires (ZnO NWs) have been successfully synthesized via a hybrid microwave-assisted sonochemical technique (HMAST) using zinc acetate dehydrate as starting material. The optimized parameters were set at 12.5 mM solution concentration and a rapid deposition time of 60 minutes. The microwave power was varied from 100 to 800 Watts and the effect of microwave power on the morphological, structural, and optical properties of

ISSN 1823-5514, eISSN 2550-164X
Received for review: 2023-01-25
Accepted for publication: 2023-06-08
Published: 2023-09-15

https://doi.org/10.24191/jmeche.v20i3.23913

the ZnO NWs has also been studied. Results showed an aligned, uniformly distributed hexagonal wurtzite structure of ZnO NWs was produced, which were augmented at 600 W microwave power, having the smallest diameter size of 29.66 nm. The XRD graph showed that the ZnO NWs produced are highly crystalline, exhibiting the sharpest and narrowest intensity of (002) peaks and a crystallite size of 18.60 nm. The transmittance spectra obtained by UV-Vis would be 89.72%, having a sharp absorption edge, implying the lower particle size of ZnO as well as exhibiting high absorbance in the ultraviolet region, indicating good crystallinity. From the findings, it can be confirmed that the microwave-assisted method helped in improving the formation of higher quality ZnO NWs that can be befittingly applied in many devices such as photocatalysts and sensors due to their excellent electrochemical properties.

Keywords: *Zinc Oxide; Nanowires; Nanostructures; Microwave-Assisted; Sonochemical*

Introduction

One of the many one-dimensional nanostructures and oxide-based multifunctional materials that are now being researched and studied is zinc oxide (ZnO), whose exceptional features can improve the performance of electrical devices as well as many other things [1]. Zinc oxide is categorized as a semiconductor in group II-VI, whose covalence is on the ionic-covalent bond semiconductor. It has a wide energy band (3.37 eV), high bond energy (60 meV), and good thermal and mechanical stability at ambient temperature, which makes it appealing for prospective usage in electronics, optoelectronics, and laser technologies [2]-[3]. Its distinct chemical properties are complemented by its straightforward crystal-growth process, which offers much cheaper production costs than those of other semiconductors utilized in nanotechnology. In addition, ZnO nanomaterials (ZnO NMs) have a diverse range of nanostructures with complex morphologies and applications [4]-[10], namely nanowires [11]-[12], nanorods [13], nanotubes [14], and nanobelts [15]. Numerous growth techniques have been reported for the synthesis of ZnO nanostructures (ZnO NSs) specifically ZnO NWs including chemical and physical techniques like thermal evaporation [16]-[18], Chemical Vapor Deposition (CVD) and cyclic feeding CVD [19]-[20], sol-gel deposition [21], [22], electrochemical deposition [12], [23]-[24], hydrothermal and solvothermal growth [25]-[30] as well as surfactant and capping agents-assisted growth [31]-[32]. It is also known that these nanostructures can be grown rather easily at low temperatures.

Though these prevalent growth methods for ZnO NWs currently practiced are mostly successful, they do, however, have a few drawbacks, such as low productivity or severe impurities from their employed assistant, also

known as a catalyst or precursor, which can cause complications for their actual nanodevice application. [33]. Another limitation would be that its usage requires severe conditions such as high temperature, high pressure, expensive materials, and complex procedures. Alternatively, microwave-assisted methods had been suggested to help overcome these challenges. The region of the electromagnetic spectrum that comprises microwaves has a wavelength (λ) between 1 mm and 1 m, which is equivalent to a frequency range between 300 MHz (λ=1 m) and 300 GHz (λ=1 mm) [34]-[35]. Its numerous benefits, including scalability, low energy consumption, quick growth, low cost, and simplicity of handling make it a highly acclaimed method to solve these concerns [36]-[39]. Moreover, in comparison to ZnO NSs synthesized using a more traditional method, the microwave-assisted process provides more control over the shape and dimensional dispersion of ZnO NSs [40]. This ensures a higher level of consistency for experimental results. In addition, microwave irradiation plays a crucial role in chemical reactions occurring in aqueous media [41], reducing the time [42] and cost, lowering particle size with a narrow size distribution, raising the product yield rate, and producing high-purity products in comparison to traditional techniques [43]-[46].

In addition, the traditional method of producing ZnO by solution-based approach mainly does not emphasize the solution preparation process but rather concentrated more on the effects of stabilizer instead of the reactant dispersion causing a non-homogeneous reaction during the mixing process of precursor and solvent which will contribute to the formation of a large particles size and reduce the surface area of the nanostructures. Through defects states such as grain boundaries, this behavior will lead to limited electron transport and a high recombination rate [47]. Hence, our research intends to optimize the aforementioned method by introducing the Hybrid Microwave-Assisted Sonochemical Technique (HMAST) while also investigating the impacts of microwave power on the overall properties ZnO NWs produced. This method incorporates a very effective and often employed solution-based method whereby the sonification process was incorporated during the mixing process, to significantly improve the interaction between the precursor and stabilizing agent and thus provide better overall control of the features of the nanostructure and further assisted by microwave irradiation to expedite the production process.

Methodology

The research approach is divided into three parts, which are outlined below. The initial step would be to prepare and clean the glass substrates. The zinc oxide nanoparticles (ZnO NPs) thin film is then prepared using an ultrasonic-assisted sol-gel spin coating process, yielding ZnO NPs array. It will next go through a microwave heating deposition process to produce ZnO NWs.

Preparation of ZnO nanoparticles seeded layer thin films

Zinc Oxide-Based Nanoparticles were prepared as a seed layer of thin films on a glass substrate which was deposited by an optimized ultrasonic-assisted sol-gel (sonochemical) spin-coating technique [48]-[49]. The sonicated sol-gel ZnO was prepared by dissolving 0.4 M zinc acetate dehydrates [$(Zn(CH_3COO)_2 \cdot 2H_2O$; Merck] which acts as the precursor in the solvent of 2-methoxy ethanol [$C_3H_8O_2$; Merck] at room temperature. Then, at 1% of aluminum nitrate nonahydrate [$Al(NO_3)_3.9H_2O$; Analar] and 0.4 monoethanolamines [MEA, C_2H_7NO; R&M] were added into the solution as dopant and stabilizer, respectively. The molar ratio of MEA to zinc acetate dehydrate was maintained at 1:1, and the resultant solution was stirred at 80 ºC for 40 minutes to yield a clear and homogeneous solution. Afterward, the solution was sonicated at 50 ºC for 30 minutes using an ultrasonic water bath (Hwasin Technology Powersonic 405, 40 kHz) and cooled to room temperature. The solution will then be used to coat the glass substrate using the spin coating technique where 10 drops of the solution were deposited onto the substrate at a speed of 3000 rpm for 30 seconds. Lastly, the samples were preheated in an atmosphere ambient at 300 ºC for 10 minutes to remove solvent and the deposition processes were repeated for the second to the fifth layer of film to achieve the required film thickness. All samples were annealed in a furnace at a temperature of 500 ºC for 1 hour.

Deposition of ZnO nanowires via hybrid microwave-assisted sonochemical technique

ZnO NWs were grown via the HMAST method. An optimized 12.5 mM concentration of the solution was prepared using Zinc acetate dehydrate [$(Zn(CH_3COO)_2 \cdot 2H_2O$; Merck] and 0.01 M hexamethylenetetramine [HMTA, $C_6H_{12}N_4$; Merck] as a precursor and stabilizer, respectively [50]. The reagents were dissolved and reacted in a beaker filled with 1000 mL distilled water as a solvent and stirred at 80 ºC for 30 minutes to yield a clear and homogeneous solution. Next, the solution was sonicated at 50 ºC for 30 minutes using an ultrasonic water bath (Hwasin Technology Powersonic 405, 40 kHz). The solution was then aged at room temperature for 1 hour and poured into a Schott bottle of 250 ml volume capacities where the optimized seed layer-coated glass substrates were placed at the bottom of the container. Afterward, the container was placed inside the 2.45 GHz microwave (SHARP 25L Microwave Oven R352ZS) which was set to a microwave power of 100 to 800 Watt for 60 minutes each. Once done, the samples were annealed at a temperature of 500 ºC for 1 hour. The procedures described above are depicted in Figure 1.

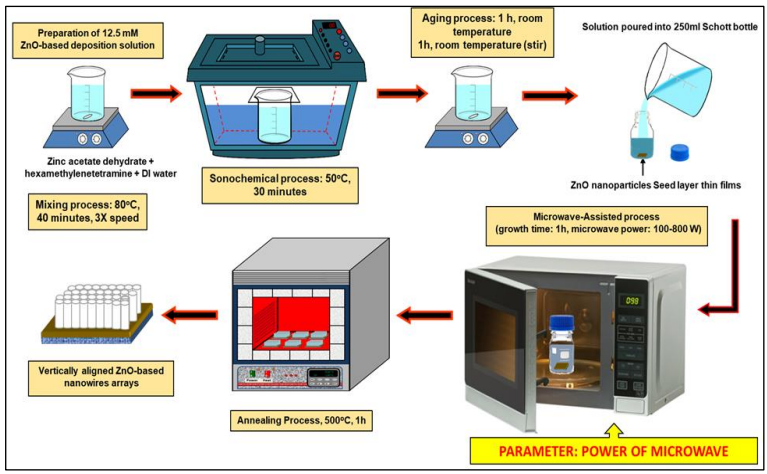

Figure 1: Deposition of ZnO NWs via a hybrid microwave-assisted sonochemical technique

Characterization method

The structural and morphological properties were characterized by X-ray diffraction (XRD, PANalytical X'Pert PRO) with Cu K-alpha radiation of a wavelength of 1.54 Å and field emission scanning electron microscope (FESEM, JEOL JSM-7600F). The optical properties were characterized by UV-visible spectroscopy (UV-Vis, Cary 5000).

Results and Discussion

Morphological and structural study

Top views of the ZnO NWs created using the HMAST approach are shown in Figure 2 which were deposited using microwave powers ranging from 100 to 800 W and an optimum solution concentration of 12.5 mM over the course of 60 minutes. It is evident that ZnO NSs were successfully produced in nanowire-type formation at the surface of the glass substrate within a very brief period of deposition time. This success may be attributed to microwave chemistry, as discussed by Abu ul Hassan et al. [51], where microwave heating provides homogeneous heat transfer to the solution mixture for chemical reactions, thereby speeding up the synthesis process.

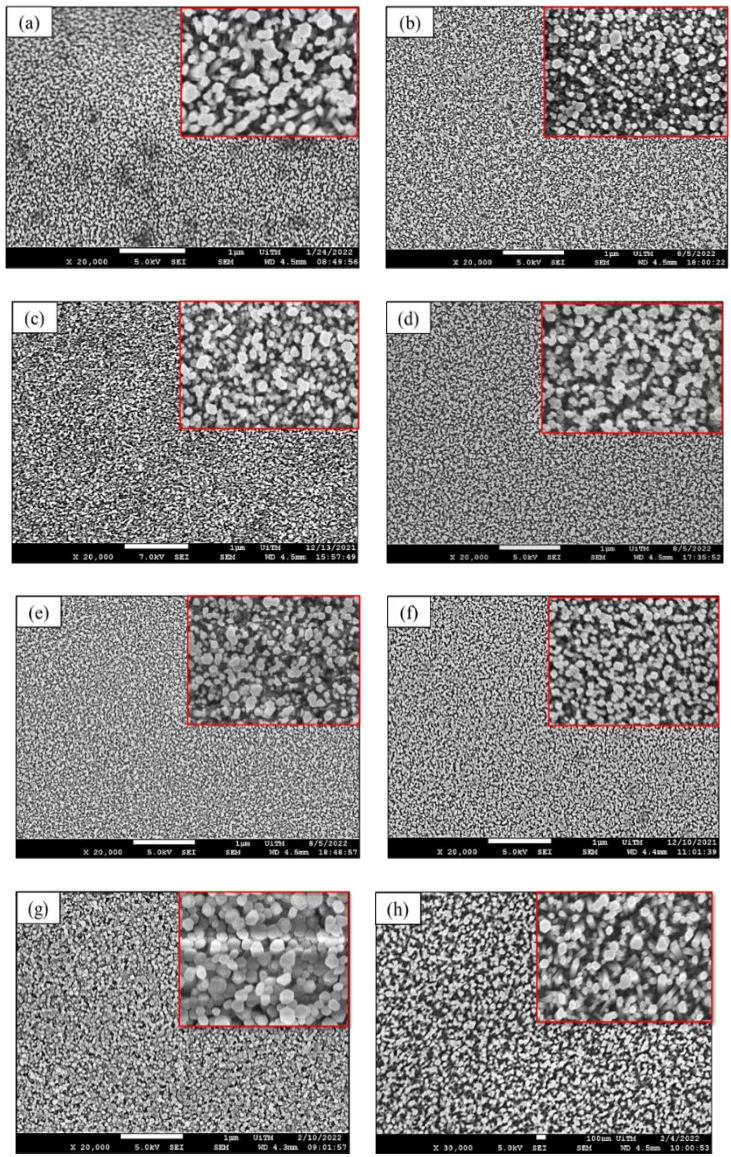

Figure 2: FESEM images of ZnO NWs by HMAST at 20000X magnification and magnified images (100000X) on the top right corner deposited at microwave power of; (a) 100 W, (b) 200 W, (c) 300 W, (d) 400 W, (e) 500 W, (f) 600 W, (g) 700 W, and (h) 800 W

In addition, compared to furnace heating, the effect of microwave growth can be seen even at relatively small microwave levels (100 W). This is explained by the reduced crystallization periods associated with the quick dissolving of precipitated hydroxides by microwave heating, as well as the rapid heating of the reaction precursors to the crystallization temperature [52]. The produced ZnO NWs have a distinct hexagonal wurtzite structure and are vertically oriented and tightly packed onto the substrate with different sizes which might be attributed to the migration rate of zinc interstitials and the vacancies are largely dependent on the change of growth temperature caused by the increase in the power of microwave [53]. Dimensions were averaged from individual nanowires according to the area distribution of nanowires from each sample where the average diameter size of the nanowires is tabulated in Table 1. It can also be observed in Figure 2(f) that the surface morphology of ZnO NWs deposited at 600 W microwave power displays the smallest diameter size and smooth uniformly distributed hexagonal NWs with a more compact structure in comparison to other samples. It is evident in Figures 2(a) to 2(f) that the nanowires' reduction in diameter size as microwave power increases from 100 to 600 W is consistent with earlier research conducted by other researchers where it was found that a higher microwave power contributes to increasing in temperature leading to the decrement in diameter size of nanostructures [54].

However, the diameter size of the nanowires starts to rise once more at power levels of 700 and 800 W as seen in Figures 2(g) and 2(h). This might be due to the microwave effect and the phenomenon of “hot spots," which is caused by the presence of zones with a higher temperature than the bulk of the aqueous solution. The maximum temperature reached in the chemical reactions during microwave heating was limited by the solution boiling temperature (105 ^{o}C for water) or higher temperature [55]. A liquid reaction mixture superheats because of these "hot spots" more than conventional heating would expect. When using a dielectric material (solid or liquid), and assuming negligible diffusion and heat losses, most of the absorbed microwave power per unit volume is converted into thermal energy within the dielectric material [56]. This is shown in the following equation where the temperature of the mixture's aqueous solution rises rapidly as the microwave power increases.

$$\frac{\Delta T}{\Delta t} = \frac{P_{abs}}{\rho C_p} = \frac{2\pi f \varepsilon_0 \varepsilon''_{eff} E^2_{rms}}{\rho C_p} = \frac{2\pi f \varepsilon_0 \varepsilon'_r tan\delta E^2_{rms}}{\rho C_p} \quad (1)$$

where ρ is the density, Cp is the specific heat capacity, ΔT is the temperature rise or the rate of heating and t is the time.

According to Debye and Stokes' theorem, the relaxation time (τ) of dipole rotation, a spherical or nearly spherical rotating dipole with radius, r is given by the following equation [57]-[58]:

$$\tau = \frac{4\pi\eta r^3}{kT} \quad (2)$$

where η is the viscosity of the medium, k is Boltzmann's constant, and T is the temperature. Relaxation data for pure water play an important role in the study of the dielectric properties of aqueous solutions [59].

On the other hand, when the temperature rises, the water phase's viscosity decreases as shown in Equation (2), increasing the possibility that water pools would collide. Water pools become less stable as a result, which raises the likelihood that ZnO nuclei will combine. As a result, ZnO nanostructures will often expand in size [60]. The change in microstructure is also explained by the Ostwald ripening theory [61].

Table 1: Structural parameters of ZnO NWs by HMAST technique deposited at various microwave power

Sample	Microwave power (W)	Peak position (2θ)	FWHM (˚)	Crystallite size (nm)	Diameter size (nm) FESEM
(a)	100	33.86	0.190	31.98	40.51
(b)	200	33.90	0.189	29.79	37.93
(c)	300	33.82	0.186	31.63	36.90
(d)	400	33.89	0.183	33.08	35.11
(e)	500	33.86	0.173	38.01	33.60
(f)	600	33.90	0.170	32.71	29.66
(g)	700	33.91	0.202	31.98	41.53
(h)	800	33.95	0.348	18.60	45.77

The results of X-ray diffraction (XRD) for these samples further supported the FESEM results where it was found that the ZnO NWs produced are in highly crystalline form and purity. Figure 3 displays the XRD patterns of the ZnO NWs thin film generated by the HMAST technique at different microwave powers of 100 to 800 W. The indexing of the various XRD peaks was carried out in accordance with the Joint Committee on Powder Diffraction Standards (JCPDS) standard database of ZnO hexagonal wurtzite nanostructure (File no. 36-1451). The ZnO NWs formed display three distinct diffraction peaks that were observed between 20 and 60 degrees, as shown in Figures 2(a) to 2(h). The observed diffracted peaks and associated *hkl* values, which were positioned along the preferred c-axis orientation and were indexed

at (100), (002), and (101), are clearly visible with varying intensities. This outcome is consistent with those mentioned in previous findings [62]-[63].

The strongest (002) orientation peak, which is evident in all samples, is between 33.82° and 33.9°, showing that the particles predominantly developed in one direction, generating structures that are almost 1D or rod-like, as can be seen by observations from all the grown samples. The weak intensities of the other peaks, on the other hand, could be caused by a few distorted alignments of ZnO NWs grown on the glass substrate. Overall, the samples that were developed exhibited clear crystalline structures and no other phase formations, including amorphous structures. Additionally, it can be noted in Figure 2(f) that ZnO NWs deposited at the maximum microwave power of 600 W exhibit the sharpest and narrowest intensity of (002) peaks as compared to ZnO NWs formed at a different microwave power of 100 to 500, 700 and 800 W. This further proves that the samples synthesized using higher microwave power have higher peak intensity, in comparison to those prepared at lower powers, indicating the increase of purity of ZnO as a function of high microwave power [64].

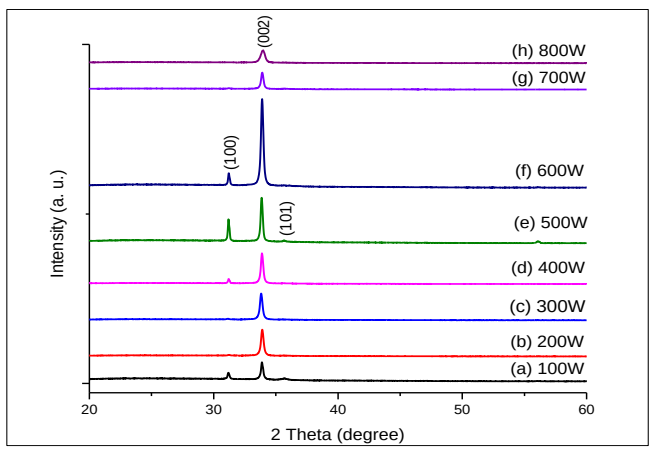

Figure 3: XRD spectra of ZnO NWs by HMAST technique deposited at various microwave power

The average crystallite sizes D (nm) of the ZnO nanowires was calculated using Scherrer's formula below.

$$D = \frac{0.9\lambda}{\beta \cos \theta} \tag{3}$$

where λ is the X-ray wavelength of Cu–Kα radiation source (=1.5418A°), β (in radians) is the full width at half maximum (FWHM) intensity of the diffraction peak located at 2θ and θ is the Bragg's angle.

Calculated results are shown and summarised in Table 1, where it is discovered that the average crystallite size increases from 45.62 to 51 nm with an increase in microwave power from 100 to 800W. Although ZnO nanowires can be grown as it is usually in the form of powders, our method opted for the use of substrates specifically low-cost soda lime silica glass as vertically oriented growth on a substrate offers significant benefits specifically for photocatalytic applications. The formation of nanowires is aided by the anisotropy of the ZnO crystal structure. The basal plane (001), with one end, in terminatively positive Zn lattice points and the other in partially negative oxygen lattice in various directions follow the pattern $\nu_{(0001)} > \nu_{(01\bar{1}\bar{1})} > \nu_{(01\bar{1}0)} > \nu_{(01\bar{1}1)} > \nu_{(000\bar{1})}$ [66].

Optical Properties

At room temperature, UV-Vis-NIR spectrophotometer measurements between 200 and 2200 nm are used to determine the optical characteristics of the ZnO NWs created by HMAST. The transmittance spectra of the ZnO NWs made using the HMAST approach are shown in Figure 4 at various microwave powers ranging from 100 to 800 W. Thin films' optical transmittance is known to be influenced by their surface shape. In this experiment, it was discovered that every sample developed met the criteria for transparency, which is above 80% in the visible-NIR range, and that the visible region's absorption edges are below 400 nm. This could be attributed to electron transitions from the valence band to the conduction band caused by the intrinsic ZnO band gap. It has also been widely reported in previous studies that the difference in particle size might be the reason for the variation in the absorption edges (67-69). Throughout the visible area, the transmittance spectra show an exciton peak in the 350-380 nm range and reduced absorbance above 380 nm. Sharp absorption edges suggest smaller ZnO particle sizes, while strong absorbance in the UV range suggests excellent crystallinity [70].

The highest transmittance was recorded for the sample synthesized at 100 W microwave power as can be seen in Figure 4(a) with an average transmittance of 95.11% between 400 nm and 800 nm in the visible region, whereas the lowest transmittance was obtained for the intrinsic sample at 700 W with an average transmittance of 83.43% over the same wavelength as seen in Figure 4(g).

It can also be seen in Table 2 that the transmittance decreases as the microwave power increases from 100 to 500 W. However, the transmittance increases again at a microwave power of 600 W with 89.72% transmittance which might be due to the homogeneous structure with uniformly distributed

particles and improvement in growth along the c-axis enhancing the optical scattering reduction in the ZnO thin films. The transmittance spectra started to decrease again at higher microwave power of 700-800 W which might be due to the change in structural properties as discussed previously. Overall, all the samples showed great transparency and it is also well known that strong transmittance properties may be used in electrical devices, such as the window layer in solar cells, to capture the most photons. Changes in the transmission spectrum were brought on by interferences in thin films caused by reflection at the air-ZnO and ZnO-glass interfaces [71].

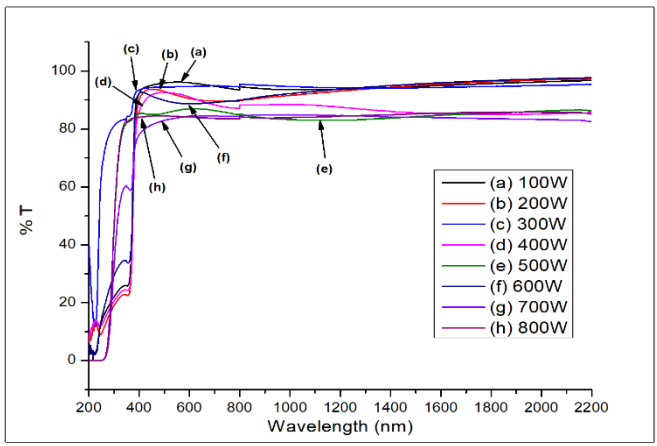

Figure 4: Transmittance spectra of ZnO NWs by HMAST technique deposited at various microwave power of (a) 100 W, (b) 200 W, (c) 300 W, (d) 400 W, (e) 500 W, (f) 600 W, (g) 700 W, and (h) 800 W as a function of wavelength

Table 2: Transmittance percentage of ZnO NWs by HMAST technique

Sample	Microwave power (W)	Average transmittance, *T* (%)
(a)	100	95.11
(b)	200	91.07
(c)	300	90.73
(d)	400	90.03
(e)	500	85.96
(f)	600	89.72
(g)	700	83.43
(h)	800	84.01

Conclusions

It can be concluded that highly crystalline ZnO NWs having hexagonal wurtzite structure with preferable c-axis orientation were successfully synthesized using a microwave-assisted sonochemical technique from 100 to 800 W of microwave power at 12.5 mM concentration and 60 minutes deposition time with profound improvement in its properties. It is found that the peak intensities of the ZnO NWs increase as the power increases up to 600 W indicating the high purity of ZnO NWs produced. The trend in the growth of the aligned ZnO NWs arrays produced is supported by the FESEM images of samples which indicate smaller diameter sizes of wires as the temperature rises with higher microwave power but starts getting bigger from 700 W of microwave power to 800 W. On the contrary, the XRD analysis obtained structural analysis which had shown significant phase identification according to JCPDS (File No 36-1451) highest intensity of (002) was observed to be very strong and narrow with bigger crystallite size at higher microwave power. The optical analysis of the samples also found that ZnO NWs obtained by this method have high transmittance of around 84% to 95.11% which is highly fitting to be applicated in electrical devices.

Contributions of Authors

The authors confirm the equal contribution in each part of this work. All authors reviewed and approved the final version of this work.

Funding

This work was supported by Grant No. 600-RMC/YTR/5/3 (005/2021) under the Ministry of Education (MOHE) and the Universiti Teknologi MARA (UiTM), Malaysia.

Conflict of Interests

All authors declare that they have no conflicts of interest

Acknowledgment

The authors would like to thank the Research Management Centre (RMC), Universiti Teknologi MARA (UiTM), Malaysia, for their support. The authors

would also like to thank Mr. Salifairus Mohammad Jafar (UiTM Senior Science Officer) and Mr. Mohd Azlan Jaafar (UiTM Assistant Engineer) for their kind support of this research.

References

[1] S. Baruah, R.F. Rafique, and J. Dutta, "Visible light photocatalysis by tailoring crystal defects in zinc oxide nanostructures", *Nano*, vol. 3, no. 5, pp. 399-407, 2008. https://doi.org/10.1142/S179329200800126X

[2] Q. Zhou, J. Z Wen, P. Zhao, and W. A. Anderson, "Synthesis of vertically aligned zinc oxide nanowires and their application as a photocatalyst", *Nanomaterials*, vol. 7, no. 1, pp. 1-13, 2017. https://doi.org/10.3390/nano7010009

[3] V. Parihar, M. Raja, and R. Paulose, "A brief review of structural, electrical and electrochemical properties of zinc oxide nanoparticles", *Reviews on Advanced Materials Science*, vol. 53, no. 2, pp. 119-130, 2018. https://doi.org/10.1016/j.ceramint.2019.11.051

[4] J. Theerthagiri, S. Salla, R. A. Senthil, P. Nithyadharseni, A. Madankumar, P. Arunachalam, T. Maiyalagan, and H. S. Kim, "A review on ZnO nanostructured materials: energy, environmental and biological applications", *Nanotechnology*, vol. 30, no. 39, pp. 1-27, 2019. https://doi.org/10.1088/1361-6528/ab268a

[5] B.G. Shohany, and A.K. Zak, "Doped ZnO nanostructures with selected elements-Structural, morphology and optical properties: A review", *Ceramics International*, vol. 46, no. 5, pp. 5507-5520, 2020. https://doi.org/10.1016/j.ceramint.2019.11.051

[6] V.S. Bhati, M. Hojamberdiev, and M. Kumar, "Enhanced sensing performance of ZnO nanostructures-based gas sensors: A review", Energy *Reports*, vol. 6, pp. 46-62, 2020. https://doi.org/10.1016/j.egyr.2019.08.070

[7] P. Vishnukumar, S. Vivekanandhan, M. Misra, and A. K. Mohanty, "Recent advances and emerging opportunities in phytochemical synthesis of ZnO nanostructures", *Materials Science in Semiconductor Processing*, vol. 80, pp. 143-161, 2018. https://doi.org/10.1016/j.mssp.2018.01.026

[8] M. Sheikh, M. Pazirofteh, M. Dehghani, M. Asghari, M. Rezakazemi, C. Valderrama, and J.L. Cortina, "Application of ZnO nanostructures in ceramic and polymeric membranes for water and wastewater technologies: a review", *Chemical Engineering Journal*, vol. 391, p. 123475, 2020. https://doi.org/10.1016/j.cej.2019.123475

[9] A. Ramirez-Canon, M. Medina-Llamas, M. Vezzoli, and D. Mattia, "Multiscale design of ZnO nanostructured photocatalysts", *Physical*

Chemistry Chemical Physics, vol. 20, no. 9, pp. 6648-6656, 2018. https://doi.org/10.1039/C7CP07984B

[10] H. Beitollahi, S. Tajik, F.G. Nejad, and M. Safaei, "Recent advances in ZnO nanostructure-based electrochemical sensors and biosensors", *Journal of Materials Chemistry B*, vol. 8, no. 27, pp. 5826-5844, 2020. https://doi.org/10.1039/D0TB00569J

[11] A. Galdámez-Martinez, G. Santana, F. Güell, P.R. Martínez-Alanis, and A. Dutt, "Photoluminescence of ZnO nanowires: a review", *Nanomaterials*, vol. 10, no. 5, pp. 1-23, 2020. http://dx.doi.org/10.3390/nano10050857

[12] C.V. Manzano, L. Philippe, and A. Serrà, "Recent progress in the electrochemical deposition of ZnO nanowires: synthesis approaches and applications", *Critical Reviews in Solid State and Materials Sciences*, vol. 47, no. 5, pp. 772-805, 2022. https://doi.org/10.1080/10408436.2021.1989663

[13] A.A. Ghassan, , N.A. Mijan and , Y.H. Taufiq-Yap, "Nanomaterials: an overview of nanorods synthesis and optimization", *Nanorods and nanocomposites*, vol. 11, no. 11, pp. 8-33, 2019. http://dx.doi.org/10.5772/intechopen.77453

[14] M.S. Lv, C. Li, Y.N. Li, X.F. Zhang, Z.P. Deng, X.L. Cheng, Y.M. Xu, L.H. Huo, and S. Gao, "Facilely controlled synthesis of porous ZnO nanotubes with rich oxygen vacancies for highly sensitive and selective detection of NO2 at low temperature", *Sensors and Actuators B: Chemical*, vol. 375, p. 132865, 2023. https://doi.org/10.1016/j.snb.2022.132865

[15] M. Hong, J. Meng, H. Yu, J. Du, Y. Ou, Q. Liao, Z. Kang, Z. Zhang, and Y. Zhang, "Ultra-stable ZnO nanobelts in electrochemical environments", *Materials Chemistry Frontiers*, vol. 5, no. 1, pp. 430-437, 2021. https://doi.org/10.1039/D0QM00709A

[16] T. Van Khai, V.M. Thanh, and T. Dai Lam, "Structural, optical and gas sensing properties of vertically well-aligned ZnO nanowires grown on graphene/Si substrate by thermal evaporation method", *Materials Characterization*, vol. 141, pp. 296-317, 2018. https://doi.org/10.1016/j.matchar.2018.04.047

[17] F.F. Alia Azmi, B. Sahraoui, and S.K. Muzakir, "Study of ZnO nanospheres fabricated via thermal evaporation for solar cell application", *Makara Journal of Technology*, vol. 23, no. 1, pp. 11-15, 2019. https://doi.org/10.7454/mst.v23i1.3644

[18] H. Ahmoum, G. Li, S. Belakry, M. Boughrara, M.S. Su'ait, M. Kerouad, and Q. Wang, "Structural, morphological and transport properties of Ni doped ZnO thin films deposited by thermal co-evaporation method", *Materials Science in Semiconductor Processing*, vol. 123, pp. 1-5, 2021. https://doi.org/10.1016/j.mssp.2020.105530

[19] P. Narin, E. Kutlu-Narin, S. Kayral, R. Tulek, S. Gokden, A. Teke, and S.B. Lisesivdin, "Morphological and optical characterizations of different ZnO nanostructures grown by mist-CVD", *Journal of Luminescence*, vol. 251, p. 119158, 2022. https://doi.org/10.1016/j.jlumin.2022.119158

[20] M. Bai, M. Chen, X. Li, and Q. Wang, "One-step CVD growth of ZnO nanorod/SnO2 film heterojunction for NO2 gas sensor", *Sensors and Actuators B: Chemical*, vol. 373, p. 132738, 2022. https://doi.org/10.1016/j.snb.2022.132738

[21] T. Amakali, L.S. Daniel, V. Uahengo, N.Y. Dzade, and N.H. De Leeuw, "Structural and optical properties of ZnO thin films prepared by molecular precursor and sol–gel methods", *Crystals*, vol. 10, no. 2, pp. 1-11, 2020. https://doi.org/10.3390/cryst10020132

[22] R. Ebrahimifard, H. Abdizadeh, and M.R. Golobostanfard, "Controlling the extremely preferred orientation texturing of sol–gel derived ZnO thin films with sol and heat treatment parameters", *Journal of Sol-Gel Science and Technology*, vol. 93, no. 1, pp. 28-35, 2020. https://doi.org/10.1007/s10971-019-05157-2

[23] F. Qiao, Q. Liang, J. Yang, Z. Chen, and Q. Xu, "A facile approach of fabricating various ZnO microstructures via electrochemical deposition", *Journal of Electronic Materials*, vol. 48, no. 4, pp. 2338-2342, 2019. https://doi.org/10.1007/s11664-019-06988-z

[24] A. Pruna, Z. Wu, J.A. Zapien, Y.Y. Li, and A. Ruotolo, "Enhanced photocatalytic performance of ZnO nanostructures by electrochemical hybridization with graphene oxide", *Applied Surface Science*, vol. 441, pp. 936-944, 2018.

[25] V. Gerbreders, M. Krasovska, E. Sledevskis, A. Gerbreders, I. Mihailova, E. Tamanis, and A. Ogurcovs, "Hydrothermal synthesis of ZnO nanostructures with controllable morphology change", *CrystEngComm*, vol. 22, no. 8, pp. 1346-1358, 2020. https://doi.org/10.1039/C9CE01556F

[26] A. Katiyar, N. Kumar, R.K. Shukla, and A. Srivastava, "Substrate free ultrasonic-assisted hydrothermal growth of ZnO nanoflowers at low temperature", *SN Applied Sciences*, vol. 2, no. 8, pp. 1-7, 2020. https://doi.org/10.1007/s42452-020-3186-1

[27] A.D. Faisal, R.A. Ismail, W.K. Khalef, and E.T. Salim, "Synthesis of ZnO nanorods on a silicon substrate via hydrothermal route for optoelectronic applications", *Optical and Quantum Electronics*, vol. 52, no. 4, pp. 1-12, 2020. https://doi.org/10.1007/s11082-020-02329-1

[28] M. Zare, K. Namratha, K. Byrappa, D.M. Surendra, S. Yallappa, and B. Hungund, "Surfactant assisted solvothermal synthesis of ZnO nanoparticles and study of their antimicrobial and antioxidant properties", *Journal of Materials Science & Technology*, vol. 34, no. 6, pp. 1035-1043, 2018. https://doi.org/10.1016/j.jmst.2017.09.014

[29] Y. Mao, Y. Li, Y. Zou, X. Shen, L. Zhu, and G. Liao, "Solvothermal synthesis and photocatalytic properties of ZnO micro/nanostructures", *Ceramics International*, vol. 45, no. 2, pp. 1724-1729, 2019. https://doi.org/10.1016/j.ceramint.2018.10.054

[30] X. Zhang, J. Chen, M. Wen, H. Pan, and S. Shen, "Solvothermal preparation of spindle hierarchical ZnO and its photocatalytic and gas sensing properties", *Physica B: Condensed Matter*, vol. 602, pp. 1-11, 2021. https://doi.org/10.1016/j.physb.2020.412545

[31] S. Zhao, Y. Shen, X. Yan, P. Zhou, Y. Yin, R. Lu, C. Han, B. Cui, and D. Wei, "Complex-surfactant-assisted hydrothermal synthesis of one-dimensional ZnO nanorods for high-performance ethanol gas sensor", *Sensors and Actuators B: Chemical*, vol. 286, pp. 501-511, 2019. https://doi.org/10.1016/j.snb.2019.01.127

[32] P. Basnet, and S. Chatterjee, "Structure-directing property and growth mechanism induced by capping agents in nanostructured ZnO during hydrothermal synthesis—A systematic review", *Nano-Structures & Nano-Objects*, vol. 22, pp. 1-24, 2020. https://doi.org/10.1016/j.nanoso.2020.100426

[33] M.N.I. Ghazali, M.A. Izmi, S.N.A. Mustaffa, S. Abubakar, M. Husham, S. Sagadevan, and S. Paiman, "A comparative approach on One-Dimensional ZnO nanowires for morphological and structural properties", *Journal of Crystal Growth*, vol. 558, pp. 1-8, 2021. https://doi.org/10.1016/j.jcrysgro.2020.125997

[34] R.T. Hitchcock, Radio-Frequency and Microwave Radiation, 3rd Edition, American Industrial Hygiene Association: Fairfax, VA, USA, 2004.

[35] M. Vollmer, "Physics of the microwave oven", *Physics Education*, vol. 39, pp. 74–80, 2004.

[36] E. Mohammadi, M. Aliofkhazraei, M. Hasanpoor, and M. Chipara, "Hierarchical and complex ZnO nanostructures by microwave-assisted synthesis: morphologies, growth mechanism and classification", *Critical Reviews in Solid State and Materials Sciences*, vol. 43, no. 6, pp. 475-541, 2018. https://doi.org/10.1080/10408436.2017.1397501

[37] C. Mallikarjunaswamy, V. Lakshmi Ranganatha, R. Ramu, and G. Nagaraju, "Facile microwave-assisted green synthesis of ZnO nanoparticles: application to photodegradation, antibacterial and antioxidant", *Journal of Materials Science: Materials in Electronics*, vol. 31, no. 2, pp. 1004-1021, 2020. https://doi.org/10.1007/s10854-019-02612-2

[38] A. Kumar, Y. Kuang, Z. Liang, and X. Sun, "Microwave chemistry, recent advancements, and eco-friendly microwave-assisted synthesis of nanoarchitectures and their applications: a review", *Materials Today Nano*, vol. 11, p. 100076, 2020. https://doi.org/10.1016/j.mtnano.2020.100076

[39] N. Devi, S. Sahoo, R. Kumar, and R.K. Singh, "A review of the microwave-assisted synthesis of carbon nanomaterials, metal oxides/hydroxides, and their composites for energy storage applications", *Nanoscale*, vol. 13, pp. 11679-11711, 2021. https://doi.org/10.1039/D1NR01134K

[40] N. Garino, T. Limongi, B. Dumontel, M. Canta, L. Racca, M., Laurenti and V. Cauda, "A microwave-assisted synthesis of zinc oxide nanocrystals finely tuned for biological applications", *Nanomaterials*, vol. 9, no. 2, pp. 1-17, 2019. https://doi.org/10.3390/nano9020212

[41] K. J. Rao, B. Vaidhyanathan, M. Ganguli, and P. A. Ramakrishnan, "Synthesis of inorganic solids using microwaves", *Chemistry of Materials*, vol. 11, no. 4, pp. 882-895, 1999.

[42] B. D. Cullity, Elements of X-ray Diffraction, Addison-Wesley Publishing, 1956.

[43] P. J. Walter, S. Chalk, and H. M. Kingston, "Overview of microwave-assisted sample preparation" in Microwave Enhanced Chemistry: Fundamentals, Sample Preparation and Applications, HM Kingston and SJ Haswell, Ed. Am. Chem. Soc., Washington, DC, pp. 55-222,1997.

[44] Y. He, "Synthesis of ZnO nanoparticles with narrow size distribution under pulsed microwave heating", *China Particuology*, vol. 2, no. 4, pp. 168-170, 2004.

[45] O. Palchik, J. Zhu, and A. Gedanken, "Microwave assisted preparation of binary oxide nanoparticles", *Journal of Materials Chemistry*, vol. 10, no. 5, pp. 1251-1254, 2000.

[46] S. Horikoshi, R.F. Schiffmann, , J. Fukushima and N. Serpone, "Materials processing by microwave heating" in Microwave Chemical and Materials Processing, Springer, Singapore, pp. 321-381, pp. 2018. https://doi.org/10.1007/978-981-10-6466-1_10

[47] M. A. Messih, M. A. Ahmed, A. Soltan, and S. S. Anis, "Synthesis and characterization of novel Ag/ZnO nanoparticles for photocatalytic degradation of methylene blue under UV and solar irradiation", *Journal of Physics and Chemistry of Solids*, vol. 135, p. 109086, 2019. https://doi.org/10.1016/j.jpcs.2019.109086

[48] M. H. Mamat, M. Z. Sahdan, Z. Khusaimi, A. Z. Ahmed, S. Abdullah, and M. Rusop, "Influence of doping concentrations on the aluminum doped zinc oxide thin films properties for ultraviolet photoconductive sensor applications", *Optical Materials*, vol. 32, no. 6, pp. 696-699, 2010. https://doi.org/10.1016/j.optmat.2009.12.005

[49] M. F. Malek, M. H. Mamat, M. Z. Musa, T. Soga, S. A. Rahman, S. A. Alrokayan and M. Rusop, "Metamorphosis of strain/stress on optical band gap energy of ZAO thin films via manipulation of thermal annealing process", *Journal of Luminescence*, vol. 160, pp. 165-175, 2015. https://doi.org/10.1016/j.jlumin.2014.12.003

[50] X. Ge, K. Hong, J. Zhang, L. Liu, and M. Xu, "A controllable microwave-assisted hydrothermal method to synthesize ZnO nanowire arrays as recyclable photocatalyst", *Materials Letters*, vol. 139, pp. 119-121, 2015. https://doi.org/10.1016/j.matlet.2014.10.058

[51] A.U.H.S. Rana, and H.S. Kim, "Growth condition-oriented defect engineering for changes in Au–ZnO contact behavior from Schottky to Ohmic and vice versa", *Nanomaterials*, vol. 8, no. 12, p. 980, 2018. https://doi.org/10.1166/jnn.2018.14971

[52] H. E Unalan, P. Hiralal, N. Rupesinghe, S. Dalal, W. I. Milne, and G. A. Amaratunga, "Rapid synthesis of aligned zinc oxide nanowires", *Nanotechnology*, vol. 19, no. 25, p. 255608, 2008.

[53] S. Rackauskas, A. G. Nasibulin, H. Jiang, Y. Tian, G. Statkute, S. D. Shandakov and E. I. Kauppinen, "Mechanistic investigation of ZnO nanowire growth", *Applied Physics Letters*, vol. 95, no. 18, p. 183114, 2009. https://doi.org/10.1063/1.3258074

[54] H. R. Rajabi, R. Naghiha, M. Kheirizadeh, H. Sadatfaraji, A. Mirzaei, and Z. M. Alvand, "Microwave assisted extraction as an efficient approach for biosynthesis of zinc oxide nanoparticles: synthesis, characterization, and biological properties", *Materials Science and Engineering: C*, vol. 78, pp. 1109-1118, 2017. https://doi.org/10.1016/j.msec.2017.03.090

[55] K. Bougrin, A. Loupy, and M. Soufiaoui, "Microwave-assisted solvent-free heterocyclic synthesis", *Journal of Photochemistry and Photobiology C: Photochemistry Reviews*, vol. 6, no. 2-3, pp. 139-167, 2005. https://doi.org/10.1016/j.jphotochemrev.2005.07.001

[56] A. Chatterjee, T. Basak, and K. G. Ayappa, "Analysis of microwave sintering of ceramics", *AIChE Journal*, vol. 44, no. 10, pp. 2302-2311, 1998. https://doi.org/10.1002/aic.690441019

[57] P. Europeˇıenne l Conseil de l'Europe, Maisonneuve S.A. Editions, Sainte Ruffine, 1996.

[58] Y.R. Naves, Technologie et Chimie des Parfums Naturels, Masson Ed., Paris, 1974.

[59] A. Loupy, and A. de la Hoz, "Microwaves in organic synthesis", John Wiley & Sons, Eds., 2013.

[60] Y. He, "Synthesis of ZnO nanoparticles with narrow size distribution under pulsed microwave heating", *China Particuology*, vol. 2, no. 4, pp. 168-170, 2004. https://doi.org/10.1016/S1672-2515(07)60050-5

[61] D. D. Dincov, K. A. Parrott, and K. A. Pericleous, "Heat and mass transfer in two-phase porous materials under intensive microwave heating", Journal *of Food Engineering*, vol. 65, no. 3, pp. 403-412, 2004. https://doi.org/10.1016/j.jfoodeng.2004.02.011

[62] N. Salah, S. S Habib, Z. H. Khan, A. Memic, A. Azam, E. Alarfaj, and S. Al-Hamedi, "High-energy ball milling technique for ZnO nanoparticles

as antibacterial material", *International Journal of Nanomedicine*, vol. 6, p. 863, 2011. https://doi.org/10.2147%2FIJN.S18267

[63] A. Azam, F. Ahmed, S. S. Habib, Z. H. Khan, and N. A. Salah, "Fabrication of Co-doped ZnO nanorods for spintronic devices", *Metals and Materials International*, vol. 19, no. 4, pp. 845-850, 2013. https://doi.org/10.1007/s12540-013-4027-1

[64] D. Papadaki, S. Foteinis, G. H. Mhlongo, S. S. Nkosi, D. E. Motaung, S. S. Ray, and G. Kiriakidis, "Life cycle assessment of facile microwave-assisted zinc oxide (ZnO) nanostructures", *Science of the Total Environment*, vol. 586, pp. 566-575, 2017. https://doi.org/10.1016/j.scitotenv.2017.02.019

[65] S. Baruah, M. A. Mahmood, M. T. Z. Myint, T. Bora, and J. Dutta, "Enhanced visible light photocatalysis through fast crystallization of zinc oxide nanorods", *Beilstein Journal of Nanotechnology*, vol. 1, no. 1, pp. 14-20, 2010. http://dx.doi.org/10.3762%2Fbjnano.1.3

[66] M. C. Medina, D. Rojas, P. Flores, E. Peréz-Tijerina, and M. F. Meléndrez, "Effect of ZnO nanoparticles obtained by arc discharge on thermo-mechanical properties of matrix thermoset nanocomposites", *Journal of Applied Polymer Science*, vol. 133, no. 30, p. 43631, 2016. https://doi.org/10.1002/app.43631

[67] C. V. Ramana, R. J. Smith, and O. M. Hussain, "Grain size effects on the optical characteristics of pulsed-laser deposited vanadium oxide thin films", *Physica Status Solidi (a)*, vol. 199, no. 1, pp. R4-R6, 2003. https://doi.org/10.1002/pssa.200309009

[68] H. Lin, C. P. Huang, W. Li, C. Ni, S. I. Shah, and Y. H. Tseng, "Size dependency of nanocrystalline TiO2 on its optical property and photocatalytic reactivity exemplified by 2-chlorophenol", *Applied Catalysis B: Environmental*, vol. 68, no. 1-2, pp. 1-11, 2006. https://doi.org/10.1016/j.apcatb.2006.07.018

[69] R. S. Yadav, P. Mishra, and A. C. Pandey, "Growth mechanism and optical property of ZnO nanoparticles synthesized by sonochemical method", *Ultrasonics Sonochemistry*, vol. 15, no. 5, pp. 863-868, 2008. https://doi.org/10.1016/j.ultsonch.2007.11.003

[70] K. P. Sridevi, S. Sivakumar, and K. Saravanan, "Synthesis and characterizations of zinc oxide nanoparticles using various precursors", *Annals of the Romanian Society for Cell Biology*, vol. 25, no. 3, pp. 8679-8689, 2021. https://www.annalsofrscb.ro/index.php/journal/article/view/2413

[71] H. Li, J. Wang, H. Liu, H. Zhang, and X. Li, "Zinc oxide films prepared by sol–gel method", *Journal of Crystal Growth*, vol. 275, no. 1-2, pp. e943-e946, 2005. https://doi.org/10.1016/j.jcrysgro.2004.11.098